

## The complex heat exchange model at growing of large alkali halide crystals

*A.V.Kolesnikov, V.I.Deshko<sup>\*</sup>, Yu.V.Lokhmanets<sup>\*</sup>,  
A.Ya.Karvatskii<sup>\*</sup>, I.K.Kirichenko<sup>\*\*</sup>*

Institute for Scintillation Materials, STC "Institute for Single Crystals", National Academy of Sciences of Ukraine, 60 Lenin Ave., 61001 Kharkiv, Ukraine

<sup>\*</sup>National Technical University of Ukraine "Kyiv Polytechnical Institute", 37 Pobedy Ave., 03056 Kyiv, Ukraine

<sup>\*\*</sup> Ukrainian Engineering Pedagogics Academy, 16 Universitetska str., 61001 Kharkiv, Ukraine

*Received June 10, 2010*

Influence of crystal and melt absorption coefficients on the growing process of large crystals of alkali halides has been studied using the numeral simulation of complex heat exchange. The developed model takes into account the radiative and conductive heat exchange in a crystal and melt in the "grey" approximation with a diffuse reflection from boundaries. The convective heat transfer is taken into account in the melt and gas atmosphere. It is shown that the change of radiation-conductive heat exchange conditions influences significantly the main technological parameters of growing process. The developed model provides an explanation for the improvement of thermal condition stability of the large crystal growth observed in experiment at increasing absorption in infrared region.

Методом численного моделирования сложного теплообмена исследовано влияние коэффициентов поглощения кристалла и расплава на процесс выращивания крупногабаритных кристаллов галогенидов щелочных металлов. Разработанная модель учитывает радиационно-кондуктивный теплообмен в кристалле и расплаве в "сером" приближении с диффузным отражением от границ. В расплаве и газовой атмосфере учитывается конвективный теплообмен. Показано, что изменение условий радиационно-кондуктивного теплообмена оказывает значительное влияние на основные технологические параметры процесса выращивания. Разработанная модель позволяет объяснить улучшение стабильности тепловых условий роста крупногабаритных кристаллов при увеличении коэффициента поглощения в инфракрасной области спектра.

### **1. Introduction**

Alkali halide crystals (AHC) are used widely as scintillators in various fields of science and engineering. On industrial scale, these crystals are grown by pulling from melt onto a seed [1, 2]. A distinctive feature of these materials is high transparency in infrared (IR) region in both crystalline [3] and molten state [4]. From viewpoint of high-quality large single crystal ingots technology, a low absorption is of a highest value, since it is just the parameter that defines the conditions of radiation-conductive heat exchange (RCHE) in a growing crystal. Experimental researches [5, 6] show that decreasing of crystal and melt transparency in IR region attained by doping with polyatomic anions, provides an improved thermal stability of the crystal growth process. At the same time, the functional characteristics of detectors made using the crystals remain essentially intact, while in some cases

[7], the doping provides a reduced afterglow level and improved radiation hardness of detectors. Studies are known [8, 9] aimed at the analysis of RCHE in a growing crystal. However, those works consider the geometrically simplified model including a cylindrical crystal only. Thus, to take into account in detail the crystal and melt optical properties influence on the thermal conditions of large AHC growth, a numerical model is to be developed taking into consideration both the complex furnace geometry and variety of heat and mass transfer mechanisms accompanying the crystal growth process.

The heat exchange processes accompanying the growth of large AHC show certain specific features. First, all the AHC are characterized by high transparency in a wide wavelength range. For example, the absorption coefficient of pure CsI crystals does not exceed  $1 \cdot 10^{-3} \text{ cm}^{-1}$  in the 0.25 to 64  $\mu\text{m}$  range [10]. Second, the external crystal surfaces are always covered with a semi-transparent condensate. It is a fine-crystalline layer of the main material with the characteristic grain size of 0.05 mm. The condensate layer thickness amounts most often 0.5 to 2 mm [11]. This work offers a model of complex heat exchange that takes into consideration those features. The problem is reduced to a two-dimensional axially symmetrical model of physical fields in the furnace including the following equations: energy (taking into account the complex heat exchange), Navier-Stokes, and radiation heat transfer in an absorptive and radiative medium.

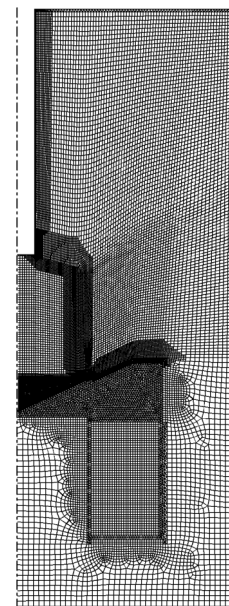


Fig.1. Computational grid.

## 2. Computational procedure

The two-dimensional axially symmetrical numerical model of heat exchange involves the areas of semitransparent crystal, melt, and gas cavities as well as the surrounding furnace elements: crucible, crystal holder, heaters, feeder, and heat insulation. The radiation-conductive heat exchange is considered in the crystal and the radiation-convective one, in the melt. In gas volumes, the convective and also radiative heat exchange is considered between the cavity walls (since the cavities are filled with monoatomic argon, the gas is not an absorption and radiation medium). To describe the convective heat transfer, the  $k-\varepsilon$  turbulence model is used. That model takes into account the rotatory motion of the crystal and crystal holder, as well as the Marangoni conditions at the free melt surface (the melt-gas interface). To calculate the radiation heat transfer, the method of discrete ordinates is used, the medium is assumed to be "grey" and isotropic, the boundaries, to be diffuse. In the energy balance at the crystal-melt interface (Stefan condition), the radiation flux is accounted for. The crystal-melt, crystal-gas and melt-gas interfaces are considered as semi-transparent. The calculation area is discretized using tetragonal and trigonal elements. To improve the convergence and increase the accuracy, the calculation network was optimized with diminution at the boundaries of areas where the liquid flow is calculated. The model was tested at different network dimensions. As a result, for reasons of minimum calculation complexity at the maintenance of necessary accuracy and convergence, the network containing 27133 two-dimensional cells was chosen. The general view of the calculation network is shown in Fig. 1.

The heat conduction equation:

$$c_p(T)\rho(T)\left[\frac{\partial T}{\partial \tau} + (\mathbf{V} \cdot \nabla)T\right] = \text{div}(\lambda(T)\nabla(T)) + E(X) + q_v(X). \quad (1)$$

Navier-Stokes equation:

$$\rho(T)\left[\frac{\partial \mathbf{V}}{\partial \tau} + (\mathbf{V} \cdot \nabla)\mathbf{V}\right] = \mu(T)\nabla^2\mathbf{V} - \nabla P + \rho(T)\mathbf{g}; \quad (2)$$

$$\nabla[\rho(T)\mathbf{V}] = 0, \quad (3)$$

where  $c_p$  is the specific isobar heat capacity, J/(kg·K);  $\rho$ , density, kg/m<sup>3</sup>;  $\mathbf{g}$ , standard gravity;  $\lambda$ , the heat conductivity coefficient, W/(m·K);  $T$ , temperature, K;  $\tau$ , time, s;  $\mathbf{V}$ , the speed vector projections on the axes  $r$  and  $z$ , m/s;  $\omega=2\pi rf$ , circular speed, m/s;  $f$ , the crystal rotation frequency, s<sup>-1</sup>;  $\mu$ , the dynamic viscosity coefficient, kg/(m·s);  $P$ , pressure, Pa;  $q_v(X)$ , the bulk density of internal heat sources, W/m<sup>3</sup>;  $E(X)$ , integral bulk density of radiation (divergence of integral radiation flow density vector), W/m<sup>3</sup>, which can be obtained from equation:

$$E(X) = \int_0^{\infty} k_v \left( 4\pi n_v^2 I_{0v} - \int_{\Omega=4\pi} I_v(\Omega) d\Omega \right) dv, \quad (4)$$

where  $k_v$  is the spectral absorption coefficient, m<sup>-1</sup>;  $n_v$ , the spectral refractive index;  $I_{0v}$ , the radiation intensity of black body given by the Plank function;  $I_v$ , spectral intensity of incident radiation as a characteristic of radiation transmission at frequency  $v$  in the direction  $\mathbf{s}$  of space angle  $\Omega$ , which depends on absorption, temperature distribution and effective radiation at a boundary;  $X = (r, z, \varphi)$ , the cylindrical co-ordinates of point for which equation is written. The radiation field in an absorptive and radiative media can be described by the transport equation:

$$\nabla \cdot [I_v(X, \mathbf{s}) \mathbf{s}] + k_v \cdot I_v(X, \mathbf{s}) = k_v \cdot n_v^2 \cdot I_{0v}. \quad (5)$$

Initial conditions at  $\tau = 0$ :

$$\begin{cases} T(r, z) = T_0 \\ \mathbf{V}(r, z) = 0 \end{cases}. \quad (6)$$

The crystal-melt interface position:

$$\Gamma_{S-L}|_{r=0} = f(r, z). \quad (7)$$

Boundary conditions at  $\tau > 0$ :

1) at the furnace outer surfaces – boundary conditions of III kind:

$$\mathbf{n} \cdot (-\lambda(T) \nabla T) = \alpha_e \rho (T - T_d); \quad (8)$$

2) at the axis — the symmetry conditions

$$\partial T / \partial r = 0; \quad (9)$$

3) at the boundaries between structural elements:

$$\begin{cases} T = 0 \\ \mathbf{n} \cdot \mathbf{q}_\lambda - q_r = 0 \end{cases}, \quad (10)$$

where  $\mathbf{q}_\lambda$ ,  $q_r$  are conductive and radiative heat fluxes respectively, W/m<sup>2</sup>;

4) at the contact boundaries between liquid and solid elements of structure (adhesion conditions):

$$\mathbf{V} = 0; \quad (11)$$

5) at free liquid-gas interfaces (thermocapillary convection, or the the Marangoni conditions)

$$\begin{cases} \mathbf{n} \cdot \tau|_L = \mathbf{n} \cdot \tau|_g + \frac{d\sigma_{ST}}{dT} \nabla T, \\ \tau = \mu(\nabla \mathbf{V} + \nabla \mathbf{V}^T) \end{cases}, \quad (12)$$

where  $\sigma_{ST}$  is surface tension, N/m;  $\tau$ , stress tensor, Pa;  $L$  and  $g$  indices are for liquid and gas, respectively.

6) Stefan condition at the phase interface:

Table 1. Thermophysical parameters for the crystal, melt, and structure elements used in the model

Thermophysical properties	Csl (cryst)	Csl (melt)	Insulation	Crucible (Platinum)	Heater (NiCr)	Steel	Ar (gas)
Heat conductivity, W/(m·K)	1.1	1	1	83	40	23	0.045
Density, kg/m <sup>3</sup>	4510	4241– 1.1834·T	1000	21500	7000	8030	Ideal gas law
Heat capacity, J/(kg·K)	201	274	200	134	450	502	520
Dynamic viscosity, (Pa·s)	–	1.7·10 <sup>-2</sup>	–	–	–	–	2.2·10 <sup>-5</sup>
Refraction index	1.7	1.5	–	–	–	–	1
Absorption, m <sup>-1</sup>	0.5; 1; 5; 10	0.5; 1; 5; 10	–	–	–	–	0

$$\left\{ \begin{matrix} T|_S = T|_L = T_m \\ \mathbf{n} \cdot \mathbf{q}_\lambda - q_r \end{matrix} \right\} = \rho_S L_f \frac{\partial \mathbf{n}}{\partial \tau} \quad (13)$$

where  $T_m$  is the equilibrium crystallization temperature, K;  $L_f$ , the latent heat of crystallization, J/kg;  $\rho_S$ , the crystal density, kg/m<sup>3</sup>.

The numerical model makes it possible to study the temperature conditions inside of the furnace, to trace gradients and thermal fluxes and character of convection development therein. Basing on calculations, the selection of necessary powers and temperatures of heaters is possible for providing of the thermal conditions of crystal growth in the KRISTALL type growth units [2] where the crystal is grown by pulling from the melt onto a seed. Thermophysical parameters for the crystal, melt, and structure elements used in the model are presented in Table.

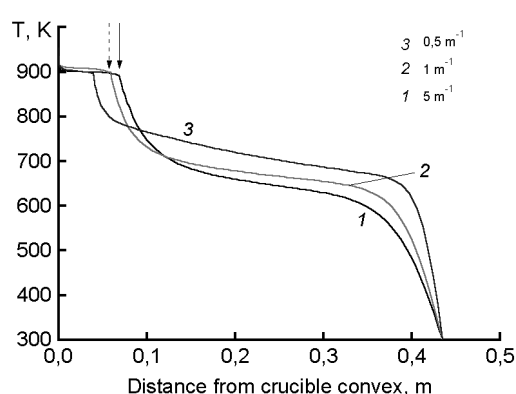


Fig.2. Axial temperature distribution in the melt and crystal at different absorption coefficients. Vertical arrow shows the interface position. 1 – 0.5m<sup>-1</sup>, 2 – 1m<sup>-1</sup>, 3 – 5m<sup>-1</sup>.

### 3. Results

Temperature distributions are calculated in the crystal and in the melt at the furnace symmetry axis at different absorption values for a 340 mm high crystal are shown in Fig. 2. Vertical arrows show the phase interface position for every absorption coefficient.

The changes in transparency of crystal and melt in IR range is seen to influence considerably the temperature distribution over the ingot volume. This influence shows itself in several aspects. At first, the increase of absorption results in a temperature rise in the head part of crystal. This evidences a radiation heat transfer from the heated bottom part of crystal and from melt to colder head part of the ingot. In this case, an additional radiation channel of heat transfer can be suggested and its effect on the crystal growth process. In the first place, this results in an additional heat removal from the interface that in accordance with the Stefan condition (16) must cause an increased crystallization speed. In such conditions, the crystal diameter automated control system compensates the increase of crystallization speed by increasing the controlling heater temperature. This explains the experimentally looked phenomenon: the AHC having high absorption coefficient grow at a continuous increase of the controlling heater temperature. In contrast, the crystals which do not contain the absorption bands in IR grow at a relatively low controlling heater temperature during the whole growing process.

#### 4. Conclusions

A two-dimensional numerical model of complex heat exchange is developed taking into account the partial absorption of heat radiation by the crystal and melt in the furnace at growing of large AHC up to 500 mm in diameter. The change of RCHE conditions influences strongly the thermal conditions of large crystal growth even at low absorption coefficients of both crystal and melt. The increase of growing crystal and melt absorption coefficients is shown to result in formation of an additional radiation channel of heat removal. This allowed to explain the experimental phenomena of improved thermal stability of growth process and pulling rate increasing at growing of crystals with an enhanced absorption.

#### References

1. V.I.Goriletsky, B.V.Grinyov, B.G.Zaslavsky et al., *Crystal Growth*, Akta, Kharkiv (2002) [in Russian].
2. B.G.Zaslavsky, *J. Cryst. Growth*, **200**, 476 (1999).
3. M.S.Pidzyraylo, I.M.Khalimonova, *Ukr. Fiz. Zh.*, **12**, 1063 (1967).
4. V.D.Golyshev, in: Proc. of 6th Int. Conf. on Single Crystal Growth and Heat & Mass Transfer, Obninsk, Russia, **4**, 738 (2005) [in Russian].
5. A.M.Kudin, B.G.Zaslavsky, S.I.Vasetsky et al., in: Proc. of 4th Int. Conf. on Single Crystal Growth and Heat & Mass Transfer, Obninsk, Russia, **1**, 176 (2001).
6. A.V.Kolesnikov, A.M.Kudin, B.G.Zaslavsky, Proc. of 6th Int. Conf. on Single Crystal Growth and Heat & Mass Transfer, Obninsk, Russia, **4**, 877 (2005) [in Russian].
7. Ukrainian Pat. 87792 C30B 15/00, C30B 15/02, C30B 29/10, G01T 1/202 (2009).
8. Yu.P.Virchenko, A.V.Kolesnikov, *Functional Materials*, **13**, 372 (2006).
9. A.V.Kolesnikov, *Functional Materials*, **14**, 164 (2007).
10. E.M.Dianov, A.I.Mitichkin, A.N.Panova et al., *Quantum Electronics*, 1345 (1980).
11. M.M.Tymoshenko, V.I.Goriletsky, V.V.Vasiliev et al., *Functional Materials*, **15**, 438 (2008).

### **Модель складного теплообміну при вирощуванні великогабаритних лужно-гаюїдних кристалів**

**О.В.Колесніков, В.І.Дешко, Ю.В.Лохманець,  
А.Я.Карвацький, І.К.Кириченко**

Методом чисельного моделювання складного теплообміну досліджено вплив коефіцієнтів поглинання кристала і розплаву на процес вирощування великогабаритних кристалів галогенідів лужних металів. Розроблена модель враховує радіаційно-кондуктивний теплообмін у кристалі та розплаві в "сірому" наближенні з дифузним відбиттям від границь. У розплаві і газовій атмосфері враховується конвективний теплообмін. Показано, що зміна умов радіаційно-кондуктивного теплообміну значно впливає на основні технологічні параметри процесу вирощування. Розроблена модель дозволяє пояснити поліпшення стабільності теплових умов вирощування великогабаритних кристалів при збільшенні коефіцієнта поглинання в інфрачервоній області спектра.